

Determination of Rigidities of Fiber-Reinforced Plastic Laminates Using Holographic Interferometry

T. Maeda* and T. Koga†
University of Tsukuba, Tsukuba 305, Japan

Introduction

FOR the conventional fiber-reinforced plastic (FRP) laminates, the bending and torsional rigidities can be calculated either according to the rule of mixture using the elastic moduli of constitutive fiber and matrix and the volume fraction, or according to the classic lamination theory (CLT) using the elastic moduli of the prepreg. However, some of the advanced composite laminates, such as carbon-carbon composites, are manufactured through a repeated process of carbonization and graphitization at high temperature, which is likely to result in a change of material properties as well as the volume fraction of the fiber and matrix. Thus, the calculation based on the virgin-material properties fails. In such a situation, the bending and the torsional rigidities must be directly evaluated from the experiment.

Laser holographic interferometry is useful for visualizing and recording the out-of-plane deflection of the whole plate. In application to a dynamic case, Aprahamian and Evensen¹ identified the mode shapes of a cantilever beam, comparing them with Timoshenko beam theory. In static cases, Yamaguchi and Saito,² and Jones and Bijl³ applied laser holographic interferometry to Cornu's method for the measurement of Poisson's ratio of isotropic plates. One of the authors developed Cornu's method to determine the ratio of the bending rigidities of orthotropic laminates.⁴ Marchant and Snell^{5,6} proposed an experimental method for determining the flexural stiffness of aluminum and carbon composite plates by using holographic interferometry. Although the validity of their method has been confirmed for specially orthotropic laminates, three rhombic test specimens must be cut from a hexagonal laminate, and the curvatures must be carefully examined.

In this study, we propose yet another measurement technique for the rigidities of the rectangular orthotropic laminates. Here, by the bending rigidities we mean D_{11} , D_{12} , and D_{22} , and by the torsional rigidity, we mean D_{66} in the following constitutive relation:

$$\begin{Bmatrix} M_x \\ M_y \\ M_{xy} \end{Bmatrix} = - \begin{bmatrix} D_{11} & D_{12} & 0 \\ D_{12} & D_{22} & 0 \\ 0 & 0 & D_{66} \end{bmatrix} \begin{Bmatrix} \partial^2 w / \partial x^2 \\ \partial^2 w / \partial y^2 \\ 2\partial^2 w / \partial x \partial y \end{Bmatrix} \quad (1)$$

The ratio of the bending rigidities (D_{12}/D_{22}) is determined from the fringe pattern of the four-point bending test. The bending rigidities (D_{11} and D_{22}) and the torsional rigidity are calculated by using the measured natural frequencies of the resonance tests. The adequacy of the present method is discussed by comparing the measured rigidities with the theoretical values obtained from CLT.

Test Specimens

Fourteen kinds of carbon FRP laminates of different composition were made, and four specimens for each composition were made. The dimensions of the plate are 270 ± 0.1 mm long by 30 ± 0.1 mm wide, and the average mass density is 1510 kg/m^3 . The composition and the thickness are listed in Table 1. The material properties used to

calculate the theoretical rigidities are $E_1 = 108 \text{ GPa}$, $E_2 = 7.34 \text{ GPa}$, $\nu_{12} = 0.326$, and $G_{12} = 3.51 \text{ GPa}$. These values were obtained from a tensile test by using the unidirectional laminates and $(\pm 45 \text{ deg})_{25}$ laminates. In the resonance test, the test specimens used in the four-point bending test were clamped at an end by a pair of steel plates to form cantilevered plates. The effective plate lengths are 180 mm for all specimens.

Four-Point Bending Test

Figure 1 shows a fringe pattern of laser holography produced by the four-point bending test. Because contour lines of pure bending deformation can be described as hyperbolas, we assume the fringe curves in the form of general hyperbolas defined by

$$x^2 + C_1x + C_2xy + C_3y^2 + C_4y + C_5 = 0 \quad (2)$$

where C_i ($i = 1, 2, 3, 4$, and 5) are constants. We set a coordinate system on the photograph of the fringe patterns, and read five coordinates on the innermost curve to determine these constants of Eq. (2). Then, the ratio of the bending rigidities can be determined using

$$D_{12}/D_{22} = (C_3 - \tan^2 \theta) / (C_3 \tan^2 \theta - 1) \quad (3)$$

where θ is given by

$$\theta = \frac{1}{2} \tan^{-1} \{C_2 / (C_3 - 1)\} \quad (4)$$

Table 1 Composition and thickness of specimens

Serial no.	Composition	Thickness, mm
1	0 deg ₁₀	2.13
2	0 deg ₈	1.70
3	0 deg ₆	1.29
4	0 deg ₂ /90 deg ₂ /0 deg ₂	1.28
5	0 deg ₂ /90 deg ₄ /0 deg ₂	1.71
6	0 deg ₂ /90 deg ₆ /0 deg ₂	2.13
7	0 deg ₄ /90 deg ₂ /0 deg ₄	2.11
8	90 deg ₁₀	2.12
9	90 deg ₈	1.70
10	90 deg ₆	1.27
11	90 deg ₂ /90 deg ₂ /90 deg ₂	1.27
12	90 deg ₂ /90 deg ₄ /90 deg ₂	1.71
13	90 deg ₂ /0 deg ₆ /90 deg ₂	2.10
14	90 deg ₄ /0 deg ₂ /90 deg ₄	2.06

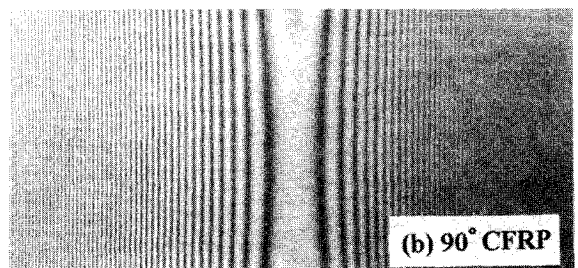
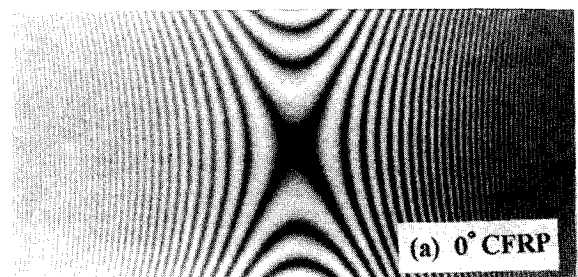


Fig. 1 Fringe patterns of bending tests.

Presented as Paper 95-1216 at the AIAA/ASME/ASCE/AHS/ASC 36th Structures, Structural Dynamics, and Materials Conference, New Orleans, LA, April 10-12, 1995; received June 2, 1995; revision received Dec. 5, 1995; accepted for publication March 13, 1996. Copyright © 1996 by the American Institute of Aeronautics and Astronautics, Inc. All rights reserved.

*Graduate Student, Institute of Engineering Mechanics. Student Member AIAA.

†Professor, Institute of Engineering Mechanics. Member AIAA.

Resonance Test

If we write the deflection in the form $w(x, y, t) = W(x, y) \sin(2\pi f t)$, Rayleigh's quotient of a cross-ply laminate having a length of a , a width of b , and a thickness of h is given by

$$(2\pi f)^2 = \frac{\int_0^a \int_0^b \{D_{11}(\partial^2 W/\partial x^2)^2 + 2D_{12}(\partial^2 W/\partial x^2)(\partial^2 W/\partial y^2) + D_{22}(\partial^2 W/\partial y^2)^2 + 4D_{66}(\partial^2 W/\partial x \partial y)^2\} dx dy}{\rho h \int_0^a \int_0^b W^2 dx dy} \quad (5)$$

where f is the frequency in Hz and ρ is the mass per unit volume.

Figure 2a shows a fringe pattern of the first bending vibration. In the first bending vibration, the lengthwise mode shape is well fit by the characteristic function of a first bending mode of a cantilever beam. The chordwise mode shape is constant. Then, we assume the function $W(x, y)$ in the form of

$$W(x, y) = A[\cosh \lambda_1 x - \cos \lambda_1 x - \alpha(\sinh \lambda_1 x - \sin \lambda_1 x)] \quad (6)$$

where $\lambda_1 = 1.875/a$, $\alpha = 0.734$, and A is an arbitrary constant.

By substituting Eq. (6) into Eq. (5), a relational expression between the bending rigidity and the natural frequency f_b of the first bending vibration can be derived:

$$D_{11} = \left(\frac{4\pi^2 \rho h}{\lambda_1^4} \right) f_b^2 \quad (7)$$

The values of D_{22} are determined by a similar test on the specimens having orthogonal composition. For example, D_{11} for the 90-deg FRP becomes D_{22} for the 0-deg FRP, and vice versa.

Figure 2b shows a fringe pattern of the first torsional vibration. In the first torsional vibration, the lengthwise and the chordwise mode shapes can be fitted approximately by linear functions. Therefore, we express the function $W(x, y)$ in the form of

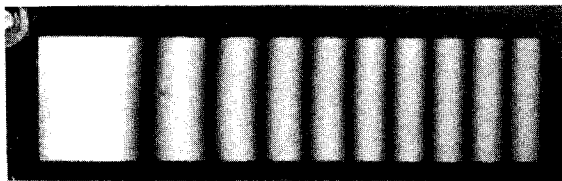
$$W(x, y) = Ax(1 - 2y/b) \quad (8)$$

By substituting Eq. (8) into Eq. (5), a relational expression between the torsional rigidity and the natural frequency f_t of the first torsional vibration is derived:

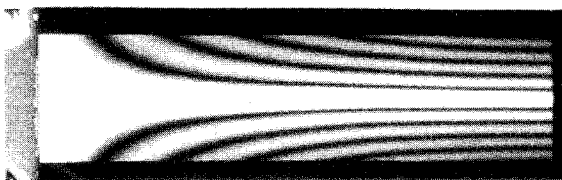
$$D_{66} = \left(\frac{\pi^2 \rho h a^2 b^2}{36} \right) f_t^2 \quad (9)$$

Results and Discussion

Figures 3 and 4 show the variation of the bending rigidities D_{11} and D_{22} with the plate thickness and with the ratio of the number of the middle 90-deg layers to the total number of layers, respectively. The experimental results are compared with the theoretical ones calculated by CLT. Both results follow a similar trend of variation, but



a) First bending vibration



b) First torsional vibration

Fig. 2 Fringe patterns of resonance tests.

there is a quantitative difference between them. The experimental results for D_{11} of thicker laminates and of 10-ply laminates having small numbers of the middle 90-deg layers are much lower than the theoretical ones. The difference is most likely attributable to

the fact that the elastic moduli used for the calculation by CLT are those obtained from a tensile test instead of those obtained from a bending test.

The bending rigidity D_{12} is determined with the aid of Eq. (3) once the bending rigidity D_{22} is determined from the resonance test and the hyperbolas of the fringe curves of the four-point bending test are identified. Results are shown in Fig. 5 as a function of the thickness together with the theoretical values calculated by CLT. The results for serial nos. (SN) 1–7 are in good agreement with the theoretical values, whereas those for SN 8–14 deviate from the theoretical ones. In the cases of SN 8–14, the fringe curves are similar to those of the 90-deg carbon FRP shown in Fig. 1b, which look more like parallel straight lines than hyperbolas. A large error is unavoidable, therefore, in identifying the hyperbolas. In cases of

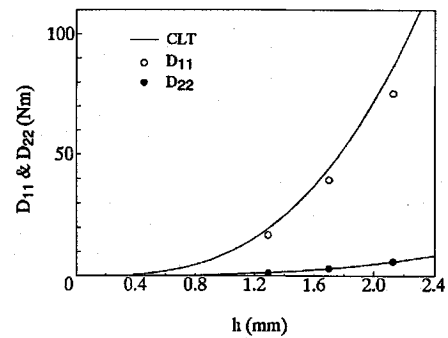


Fig. 3 Comparison of bending rigidities: 0-deg carbon FRP.

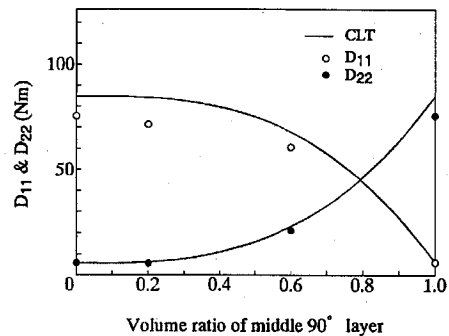


Fig. 4 Comparison of bending rigidities: 10-ply carbon FRP.

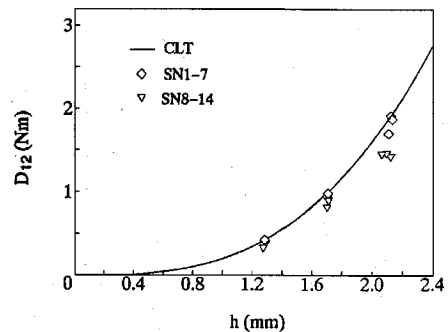


Fig. 5 Comparison of bending rigidity.

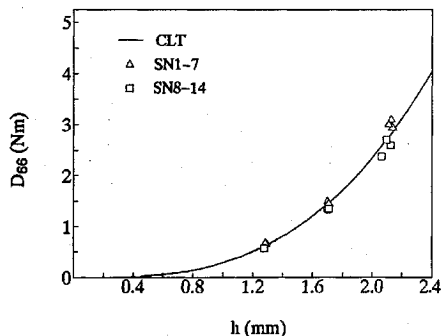


Fig. 6 Comparison of torsional rigidity.

SN 1–7, on the other hand, the fringe curves look like hyperbolas, as those shown in Fig. 1a, and the identification is more accurate.

The variation of the torsional rigidity with the plate thickness is shown in Fig. 6. The measured values are in good agreement with the theoretical values.

Conclusions

In this Note, we present a measurement technique for the bending rigidities D_{11} , D_{22} , and D_{12} and the torsional rigidity D_{66} of FRP laminates by using laser holographic interferometry. The adequacy of the method is confirmed by a comparison of the experimental result obtained by this method with the theoretical results calculated by CLT. The method is most useful for the measurement of the

torsional rigidity D_{66} , because there is no other simple but accurate method available. Judging from the good result of the torsional rigidity, our attempt at using linear functions as the lengthwise and the chordwise mode shapes has been successful.

Acknowledgment

We wish to express our thanks to Hiromitsu Otsuka of the National Institute of Biotechnology and Human-Technology of the Ministry of International Trade and Industry for his aid in the tensile test.

References

- ¹Aprahamian, R., and Evensen, D. A., "Applications of Holography to Dynamics: High-Frequency Vibrations of Beams," *Journal of Applied Mechanics*, Vol. 37, June 1970, pp. 287–291.
- ²Yamaguchi, I., and Saito, H., "Application of Holographic Interferometry to the Measurement of Poisson's Ratio," *Japanese Journal of Applied Physics*, Vol. 8, June 1969, pp. 768–771.
- ³Jones, R., and Bijl, D., "A Holographic Interferometric Study of the End Effects Associated with the Four-Point Bending, Technique for Measuring Poisson's Ratio," *Journal of Physics E: Scientific Instruments*, Vol. 7, 1974, pp. 357, 358.
- ⁴Kato, Y., and Koga, T., "Optical Measurement of Elastic Constants of Orthotropic Laminates," *Journal of the Japan Society for Aeronautical and Space Sciences*, Vol. 38, July 1990, pp. 362–370 (in Japanese).
- ⁵Marchant, M. J., and Snell, M. B., "Determination of the Flexural Stiffness of Thin Plates from Small Deflection Measurements Using Optical Holography," *Journal of Strain Analysis*, Vol. 17, No. 1, 1982, pp. 53–61.
- ⁶Snell, M. B., and Marchant, M. J., "Determination of the Flexural Stiffness of Carbon Composite Plates by Holographic Interferometry," *Journal of Strain Analysis*, Vol. 19, 1984, pp. 249–259.